

ORIGINAL COMMUNICATION

Internal Rib Structure can be Predicted Using Mathematical Models: An Anatomic Study Comparing the Chest to a Shell Dome With Application to Understanding Fractures

AARON R. CASHA,^{1,2*} LIBERATO CAMILLERI,³ ALEXANDER MANCHÉ,² RUBEN GATT,⁴ DAPHNE ATTARD,⁴ MARILYN GAUCI,⁵ MARIE-THERESE CAMILLERI-PODESTA,¹ STUART MCDONALD,⁶ AND JOSEPH N. GRIMA⁴

¹Department of Anatomy, University of Malta, Msida, Malta

²Department of Cardiothoracic Surgery, Mater Dei Hospital, Msida, Malta

³Department of Statistics and Operations Research, Faculty of Science, University of Malta, Msida, Malta

⁴Metamaterials Unit, Faculty of Science, University of Malta, Msida, Malta

⁵Department of Anesthesia, Mater Dei Hospital, Msida, Malta

⁶Department of Human Biology, School of Life Sciences, College of Medicine Veterinary and Life Sciences, University of Glasgow, United Kingdom

The human rib cage resembles a masonry dome in shape. Masonry domes have a particular construction that mimics stress distribution. Rib cortical thickness and bone density were analyzed to determine whether the morphology of the rib cage is sufficiently similar to a shell dome for internal rib structure to be predicted mathematically. A finite element analysis (FEA) simulation was used to measure stresses on the internal and external surfaces of a chest-shaped dome. Inner and outer rib cortical thickness and bone density were measured in the mid-axillary lines of seven cadaveric rib cages using computerized tomography scanning. Paired *t* tests and Pearson correlation were used to relate cortical thickness and bone density to stress. FEA modeling showed that the stress was 82% higher on the internal than the external surface, with a gradual decrease in internal and external wall stresses from the base to the apex. The inner cortex was more radio-dense, $P < 0.001$, and thicker, $P < 0.001$, than the outer cortex. Inner cortical thickness was related to internal stress, $r = 0.94$, $P < 0.001$, inner cortical bone density to internal stress, $r = 0.87$, $P = 0.003$, and outer cortical thickness to external stress, $r = 0.65$, $P = 0.035$. Mathematical models were developed relating internal and external cortical thicknesses and bone densities to rib level. The internal anatomical features of ribs, including the inner and outer cortical thicknesses and bone densities, are similar to the stress distribution in dome-shaped structures modeled

*Correspondence to: Dr. Aaron Casha, Department of Cardiothoracic Surgery, Mater Dei Hospital, Msida MSD 2090, Msida, Malta. E-mail: aaron.casha@um.edu.mt

Received 16 June 2015; Revised 14 August 2015; Accepted 18 August 2015

Published online 2 September 2015 in Wiley Online Library (wileyonlinelibrary.com). DOI: 10.1002/ca.22614

using FEA computer simulations of a thick-walled dome pressure vessel. Fixation of rib fractures should include the stronger internal cortex. *Clin. Anat.* 28:1008–1016, 2015. © 2015 Wiley Periodicals, Inc.

Key words: rib; biomechanics; measurement; morphology; Wolff's Law; Laplace Law

INTRODUCTION

The chest has been considered to behave as a thin-walled pressure vessel, since coughing causes a distending pressure with stress, defined as force across an area, to develop in the chest wall (Casha et al., 2012). The degree of stress depends on location within the thorax (Pender, 2009), but is roughly proportional to the radius at a tangent to the curvature (Young and Budynas, 2002), with larger radii developing higher stresses. Thin-walled pressure vessels have negligible mass (Pontrelli, 2002), but the chest has a self-supporting mass and the clavicles transfer some of the weight of the upper limbs to the chest wall; also, a portion of the weight of the neck and head is transferred to the thorax, though most of this weight passes through the vertebral column (Pal and Routal, 1986, 1987).

The chest resembles a hollow ellipsoid shell in shape (Casha et al., 2014) (Fig. 1) and can also be considered as a load-bearing shell structure, or dome, implying advantages of low weight and high strength (Huerta, 2006). Domes show self-supporting stability, and structurally withstand vibration and perforation well, and these advantages are enhanced by double-shelled dome construction (Ashkan and Ahmad,

2010). The inner and outer rib cortices within the rib cage can be considered to resemble the structure of a double-shelled dome, with the upper and lower cortices acting as struts linking the two shells.

Wolff's Law states that bone adapts its architecture to loads (Huiskes, 2000). Bone stress results in increases of both cortical thickness (Bass et al., 2002; Robling et al., 2002) and bone density (Cadet et al., 2010). The hypothesis that the chest behaves as a dome implies that the rib cage should show variations in cortical thickness and bone density that mimic the stresses present in the FEA model, the differing levels of force at various sites within the chest influencing the composition and architecture of the bone (Ruff et al., 2006).

The aim of this biomechanical study is to produce a more realistic and accurate thick-walled finite element analysis (FEA) model of the chest to measure chest wall stresses in order to assess whether the internal anatomical features of ribs, including the inner and outer cortical thicknesses and bone densities, are similar to the stress distribution in dome structures; previous analyses have investigated a simpler thin-walled pressure vessel model of the chest (Casha et al., 2015).

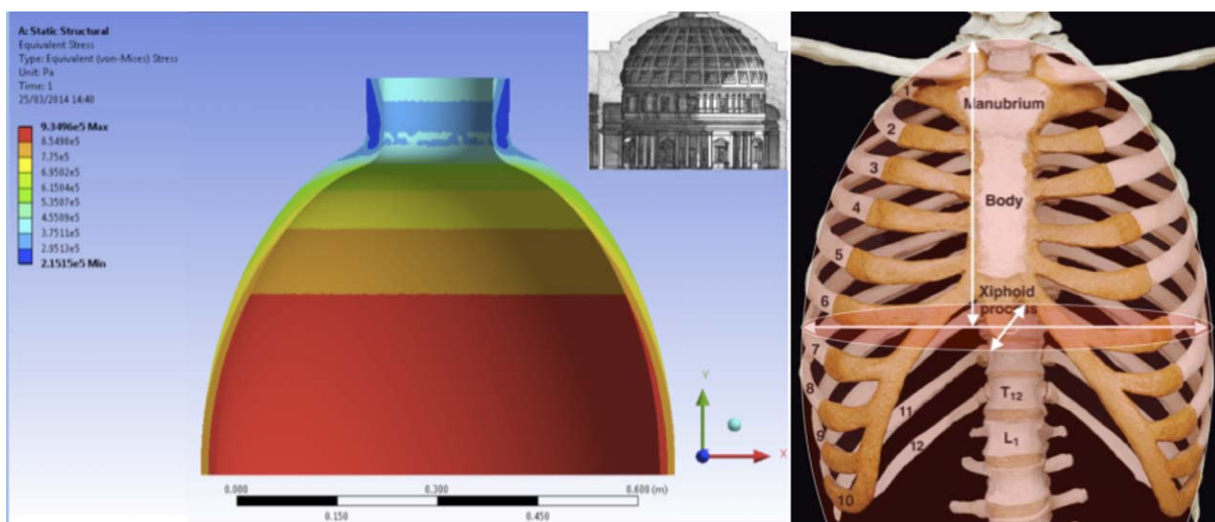


Fig. 1. Coronal view of a spheroidal FEA model and Parthenon (inset). An analogy is drawn between domes and the FEA shell structure in a hypothetical round chest. Whilst high stress is represented on the FEA model as a color scale, it leads to a greater thickness of the dome's wall. [Color figure can be viewed in the online issue, which is available at wileyonlinelibrary.com.]

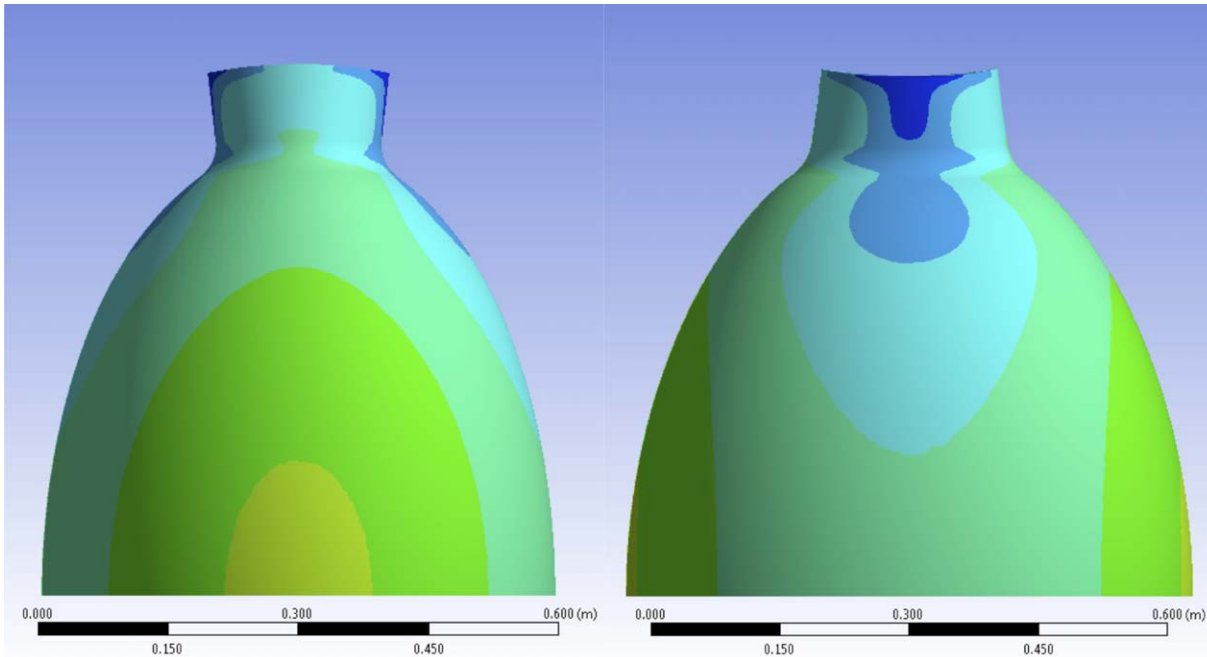


Fig. 2. Front and side elevations of the ellipsoid FEA model showing surface von Mises stress levels. [Color figure can be viewed in the online issue, which is available at wileyonlinelibrary.com.]

METHODS

Finite Element Analysis (FEA) Model

An ellipsoid with coronal radius 12 cm, sagittal radius 11 cm, vertical height 21 cm, and thickness 2 cm was used to produce a finite element analysis (FEA) computer model. This model, based on published methods using the mean dimensions of seven rib cages that were statistically significantly similar to an ellipsoid with the above dimensions, mimicked the front and side of the chest above the widest point of the rib cage, the equator of the ellipsoid being equivalent to the widest part of the cage between the sixth and seventh ribs (Casha et al., 2014; Casha et al., 2015) (Fig. 2). Ansys® software version 12 (Ansys, Canonsburg, USA) was used for FEA modeling, with scripting in ADPL language (ANSYS Parametric Design Language). The ellipsoid shell model was constrained at its base and subjected to a 40 kPa internal distending pressure (Talbert, 2005), and stress was measured at the internal and external surfaces of the shell in the mid-axillary line. The top of the model was loaded with a nominal 1 kg mass to simulate the minimal axial loading by the weight of the head and neck, since most of the weight passes through the vertebral column (Pal and Routal, 1986, 1987).

Rib Cortical Thickness and Density

High resolution CT scans of seven rib cages from anonymized cadavers were analyzed using Osirix image processing software (Osirix, Pixmeo,

Switzerland), and two types of measurement were performed (Fig. 3):

- A. Maximal rib cortical thickness. The thicknesses of the inner and outer rib cortices were measured at the mid-axillary line of the specimen, choosing the widest rib cortex located by a concurrent three-planar view in all three axes on the CT scan software.
- B. Maximal rib cortical radio-density measurements of pixel density in hounsfield units (HU) of the inner and outer rib cortices at the mid-axillary line. The radio-density was taken as a marker of the level of calcification within the bone. The mid-axillary line location was chosen because it allowed measurements with the FEA model to be located accurately.

Statistics

Paired *t* tests were used to compare inner versus outer cortical thicknesses and bone densities. Pearson correlation was used to measure the strength of the relationships between inner cortical thickness and bone density with internal stress, and similarly outer cortical thickness and bone density with external stress. Quadratic regression models were used to relate inner and outer cortical thickness and bone density to rib level. Parameters were estimated using the maximum likelihood method and goodness of fit was measured using the *R*-square value.

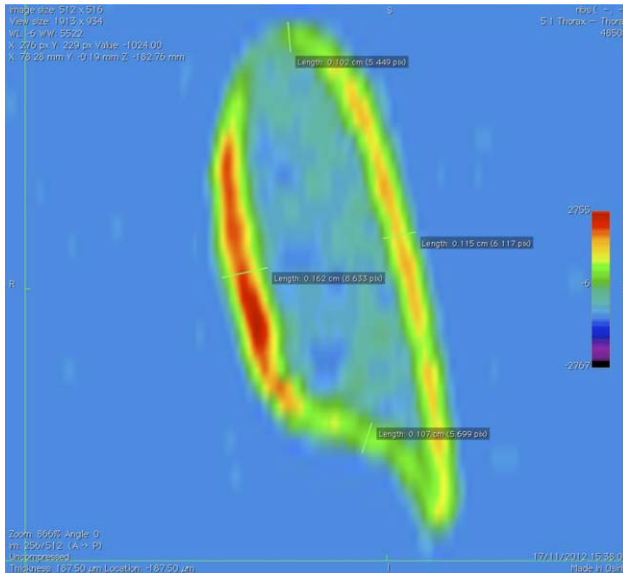


Fig. 3. Sixth rib cortical thickness measurements in coronal section at the mid-axillary line taken at the internal and external cortices on CT scan. The method used was similar to that of Mohr (2007). The resolution of CT scanning is high in the transverse plane but limited in the axial plane by the mechanics of a 0.25 mm helical pitch. [Color figure can be viewed in the online issue, which is available at wileyonlinelibrary.com.]

TABLE 1. Measurements of Internal and External Wall Stresses for the FEA Model With a Neck With an Ellipsoid Chest Shape With Coronal Radius 12 cm, Sagittal Radius 11 cm, and Vertical Height 21 cm

Rib level	Wall stress $\times 10^5$ Pa	
	Internal	External
2.0	9.85	2.90
2.5	9.78	3.92
3.0	9.96	4.62
3.5	10.19	5.09
4.0	10.40	5.40
4.5	10.58	5.64
5.0	10.72	5.80
5.5	10.82	5.91
6.0	10.89	5.99
6.5	10.88	5.99

Results

FEA model wall stress. FEA modeling of the chest showed that the stress at the base (equator) was 6×10^5 Pa externally and 10.9×10^5 Pa internally, an increase of 82% from the non-pressure-bearing external surface to the pressure-bearing internal surface. There was a gradual increase in internal and external wall stresses from the level below that of the first rib down to the equator of the ellipsoid chest (Table 1 and Fig. 4).

Radio-density and cortical thickness. Ribs respond to stress with means of a 29% external

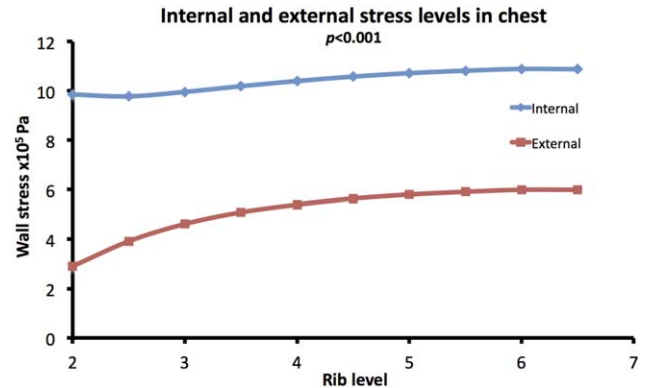


Fig. 4. Von Mises stresses at internal and external surfaces of the lateral aspect of chest, showing higher stress internally than externally. [Color figure can be viewed in the online issue, which is available at wileyonlinelibrary.com.]

cortical and 55% internal cortical increase in thickness, and a 35% external and 53% internal increase in density, between the 3rd and 7th rib levels (Fig. 5). The 7th–9th rib levels in Figure 5 behave as mirror images of the 4th–6th rib levels, similar to the ellipsoid model superimposed on the rib cage, illustrated in Figure 1. In contrast, the one fetal skeleton examined had uniform cortical thickness, indicating that changes in rib cortical thickness and radio-density occur during development.

The inner cortex was more radio-dense ($P < 0.001$) than the outer cortex with a gradual increase in both cortices with increasing rib level, reaching a maximum at the widest part of the chest wall (around the 7th rib), reducing again in the lower ribs (Fig. 6). Cortical rib thickness was measured using fine section CT cuts and the inner cortex was thicker than the outer ($P < 0.001$), the inner averaging 1.5 mm in thickness whilst the outer was about 1-mm thick.

Statistics

Graphs displaying measurements of cortical thickness and bone density against rib level suggested that quadratic regression models would provide a better fit than linear ones. The large dispersion in the data could probably be attributed to the different sizes and weights of our anonymized subjects. A quadratic regression model following the form of the general quadratic equation $y = ax^2 + bx + c$, relating the mean measurements of cortical thickness and bone density to rib level, provided the best R -square values. Most of the quadratic model parameters (a , b , and c) estimated by maximum likelihood reached statistical significance with P values < 0.05 . All the estimated regression coefficients for a were negative, implying maximum turning points, as displayed in Figure 7.

The statistical models (Table 2) suggested that the external rib cortex was exposed to very attenuated stress levels, in agreement with the thick-walled pressure vessel model in which the gradient in radial stress diminishes externally.

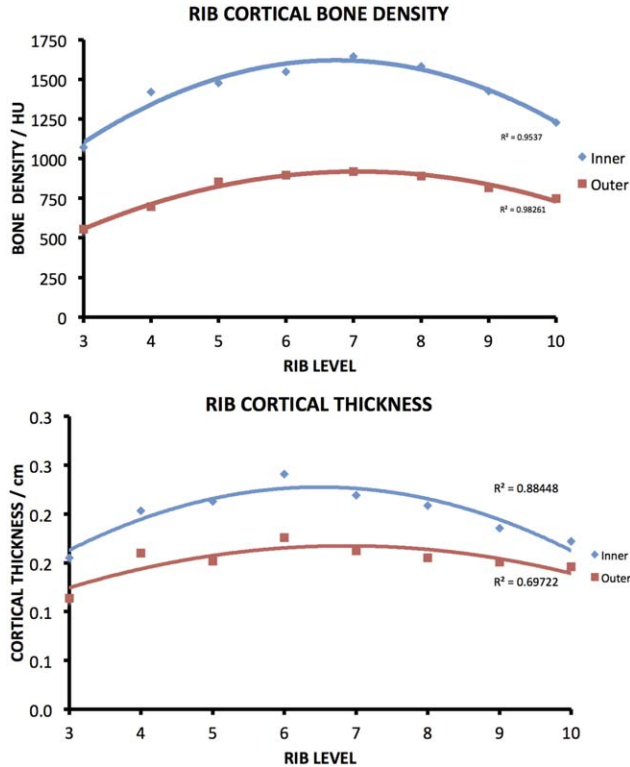


Fig. 5. Graphs showing mean rib internal and external rib cortical bone densities (A) and thicknesses (B) at different rib levels for seven specimens, with significant differences between internal and external cortical densities and thicknesses respectively, *t* test $P < 0.001$, and maximum values between the sixth and seventh ribs. [Color figure can be viewed in the online issue, which is available at wileyonlinelibrary.com.]

The four quadratic regression models are: predicted inner cortical thickness = $-0.0028x^2 + 0.0320x + 0.1256$ predicted outer cortical thickness = $-0.0014x^2 + 0.0176x + 0.1074$ predicted inner cortical density = $-16.60x^2 + 209.21x + 862.59$ predicted inner cortical density = $-9.35x^2 + 136.26x + 604.21$ where x is the rib number. Paired *t* tests showed statistically significant differences between inner and outer cortical thicknesses, $P < 0.001$, and inner and outer bone densities, $P < 0.001$. The Pearson coefficient showed a significant correlation between inner cortical bone density and internal stress, $r = 0.87$, $P = 0.003$, inner cortical thickness, and internal stress, $r = 0.94$, $P < 0.001$, and outer cortical thickness and external stress, $r = 0.65$, $P = 0.035$. The outer cortical bone density failed to reach statistical significance against external stress, $r = 0.56$, $P = 0.073$, perhaps because of the predicted attenuated external stress levels according to the FEA model.

DISCUSSION

Architectural domes are load-bearing shells (Misztal, 2010), and can be divided into single- and double-

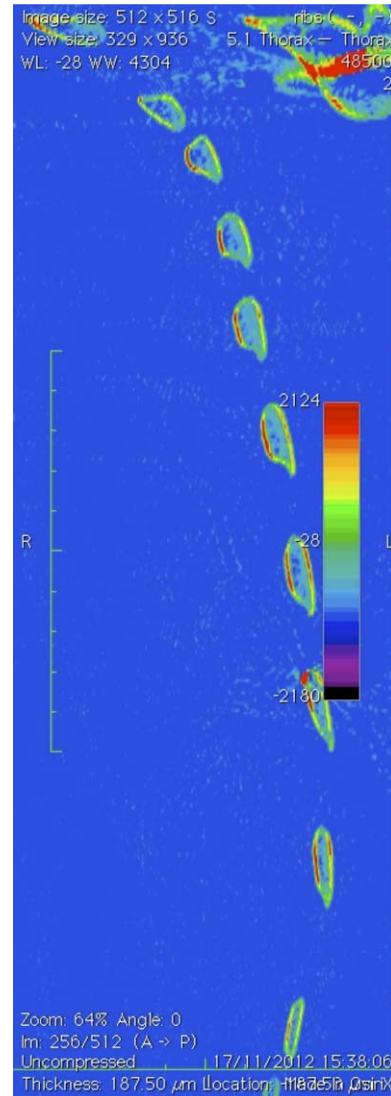


Fig. 6. High resolution CT scan of the rib cage at the mid-axillary line with a color look-up table (CLUT) with the Hounsfield Unit (HU) scale. The red coloration is predominant at the internal rib cortical surface as opposed to the external surface. [Color figure can be viewed in the online issue, which is available at wileyonlinelibrary.com.]

shell constructions (Ashkan and Ahmad, 2010). As will be discussed below, the double-shell construction, although more complex, has certain advantages over the single-shell construction particularly because less building material is used, resulting in a lower weight without sacrificing strength or rigidity (Hillenbrand, 1994), elements that are especially important for both moving creatures and architectural structures. It must be emphasized that the engineering of these structures is still not fully understood, and the two domes have ties between them that bind them into a single composite construction (Ashkan and Ahmad, 2010).

The term "double-shell dome" implies two independent concentric structures, but this is an

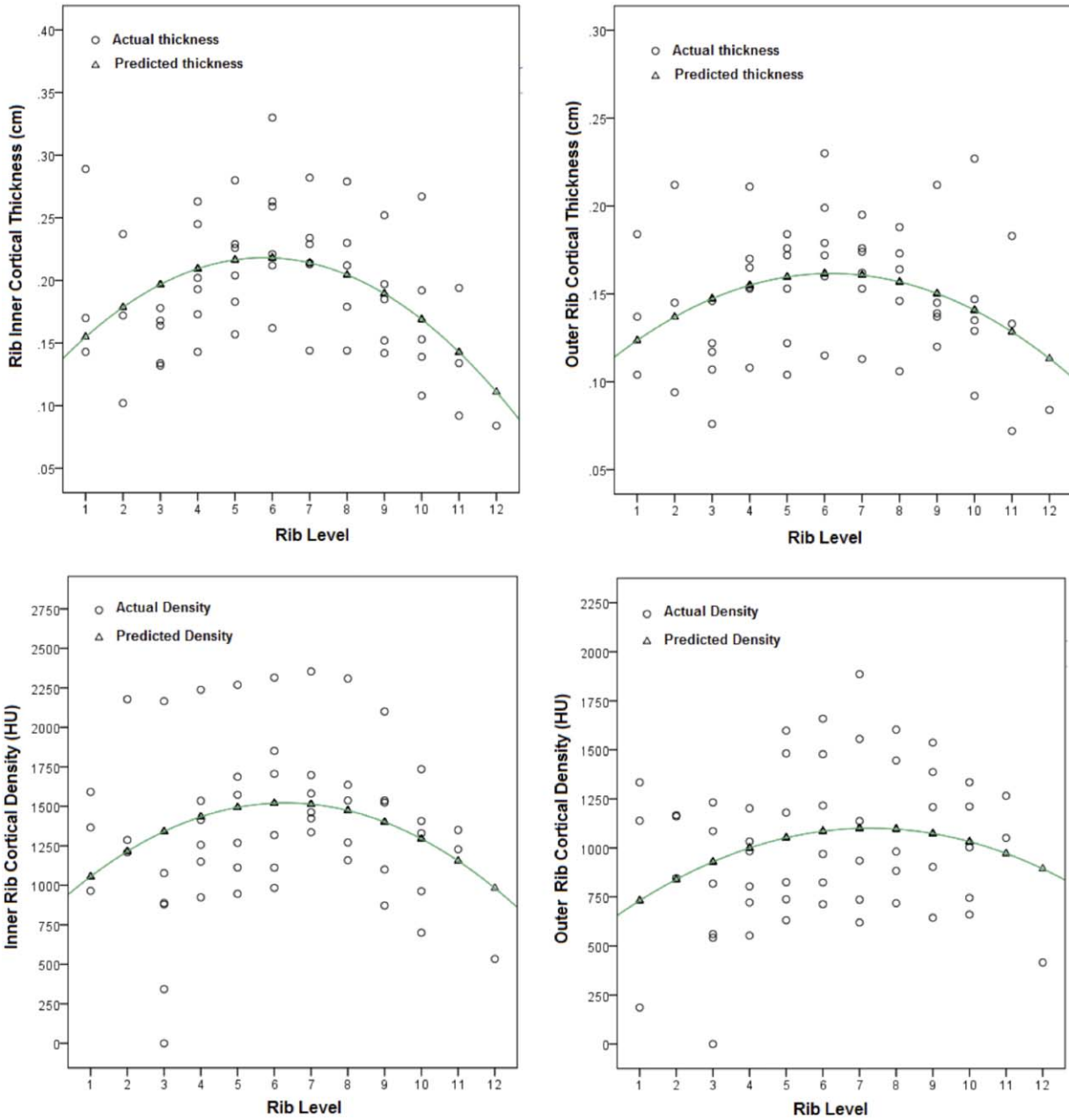


Fig. 7. Scatter plots displaying actual and predicted inner and outer rib cortical thickness and bone density values. [Color figure can be viewed in the online issue, which is available at wileyonlinelibrary.com.]

oversimplification: there are in fact three structures since the inner and outer layers are tied together by a series of interconnecting struts. These can be placed as horizontal rings but also as vertical ribs, so the middle layer resembles a mesh or spacer of wine-rack appearance that provides cross-bracing between the inner and outer shells, increasing the strength and rigidity of the structure in a sandwich or composite fashion with the middle layer acting as honeycomb.

The main advantage of a double dome is its weight and strength (Michell, 1978). The inner dome is typically load-bearing as this is more efficient, the stresses being maximal on the inner aspect. The outer dome has a supporting role and acts to stiffen the structure, therefore increasing its stability (Farshad, 1977; Hejazi, 2003). One aspect of this construction is that the inner dome is thicker than the outer one, and there is tapering from bottom to top, the bottom being thicker in both the inner and outer domes.

TABLE 2. Four Quadratic Regression Models can be Used to Predict Inner/Outer Cortical Thickness/ Bone Density (y) Given the Rib Level (x)

Model for parameter estimates	R-square	Parameter	Estimate	Standard error	P values	95% Confidence interval	
						Lower bound	Upper bound
Inner cortical thickness with rib level	0.213	a	-0.0028	0.0008	0.001	-0.0043	-0.0012
		b	0.0320	0.0100	0.002	0.0119	0.0522
		c	0.1256	0.0288	< 0.001	0.0678	0.1834
					$y = -0.0028x^2 + 0.0320x + 0.1256$		
Outer cortical thickness with rib level	0.105	a	-0.0014	0.0006	0.024	-0.0026	-0.0003
		b	0.0176	0.0075	0.023	0.0025	0.0326
		c	0.1074	0.0214	<0.001	0.0644	0.1505
					$y = -0.0014x^2 + 0.0176x + 0.1074$		
Inner cortical density with rib level	0.081	a	-16.60	7.88	0.040	-32.43	-0.77
		b	209.21	100.02	0.041	8.41	410.01
		c	862.59	282.26	0.004	295.92	1429.25
					$y = -16.60x^2 + 209.21x + 862.59$		
Outer cortical density with rib level	0.068	a	-9.35	6.07	0.129	-21.54	2.84
		b	136.26	77.02	0.083	-18.37	290.88
		c	604.21	217.36	0.007	167.85	1040.58
					$y = -9.35x^2 + 136.26x + 604.21$		

The table gives parameter estimates for a, b, and c and their 95% confidence intervals, standard errors, P values and R-square values for each quadratic model.

Another advantage is that a dome is a self-supporting structure, and one break in it does not reduce stability such that the structure collapses, which is an important property in the context of thoracic trauma.

The ribs can be considered part of a double-shell composite material dome, like a masonry dome. The middle layer of the double-shell dome acts as a honeycomb, formed by the medullary bone and the upper and lower rib cortices. Together, they act as inter-connectors binding the inner and outer cortices together. Ribs are embedded in the internal aspect of the chest wall, as this is a more advantageous position in terms of rigidity in a pressure vessel than the external aspect, since radial stress is higher internally and decreases externally. In thin-walled pressure vessels, radial stress is assumed to be zero (Parnas and Katirci, 2002), and although the chest simulates a thin-walled pressure vessel in that the radius to thickness ratio approaches 10:1 (Casha et al., 2012), a thick-walled model remains more accurate (Young and Budynas, 2002).

The cortical thickness and bone mineral density of ribs vary such that both thickness and density are maximal at the widest part of the ellipsoid human chest and taper toward the lower ribs and the third rib. The inner rib cortical thickness and bone density were significantly related to internal stress in a thick-walled ellipsoid FEA pressure vessel, $P < 0.001$ and $P = 0.003$, whilst the outer rib cortical thickness was significantly related to external stress, $P = 0.035$, the inner cortex being more radio-dense, $P < 0.001$, and thicker, $P < 0.001$, than the outer. These results are consistent with the FEA modeling, which showed that internal stress was 82% higher than external stress at the base, with a gradual decrease in both internal and external wall stresses from the base to the apex. As the stress in a pressure vessel varies according to location within the vessel, with forces approximately proportional to the radius of curvature, different ribs are exposed to different stresses depending on level.

Ribs respond to these stresses by increasing their cortical thickness and bone mineral density from the initial state in the one neonate skeleton examined, where all ribs were identical.

Ribs act as beams or columns that are pivoted at both ends. The tissues of the chest wall act to give lateral rigidity to these struts in the plane of the wall. The stability of the arrangement of the ribs is similar to that of domes. Domes can be considered as a series of arches, stability being inherent in their arch subunits; that is, they can easily withstand relative movement of the supporting walls and allow cracks to develop without collapsing—one reason why domes can survive piercing and resist seismic activity. These qualities inherent in a dome would be useful when an animal injures itself, as injury to a rib would not cause complete loss of function.

The stability of any strut under load depends on the length of the column, its width, the magnitude of the load exerted upon it, and the angulation of this load, according to Leonhard Euler's formula for the critical buckling load of an ideal strut, derived in 1757. Also important are the conditions under which the ends of the strut are fixed. Considering the ribs as struts, they are fixed at the vertebral and sternal ends. The vertebral end has the costo-vertebral joint, which is held in place at three levels—the head, the neck, and the tubercle of the rib—and is pinned to the transverse process of the vertebra so that only slight movement is possible. The anterior (sternal) end is attached via primary cartilaginous joints to the costal cartilages and is also effectively pinned. Because both ends are pegged with minimal rotation, ribs have excellent stability according to Euler's formula (Dai and Liu, 1992), with a maximal K-value, or effective strut length factor, of two to four, a higher K-value (range 0–4) indicating greater stability and resistance to buckling. This enables ribs to function more efficiently as struts or columns, and consequently to be more lightweight.

The differing directions of the inner and outer intercostal muscles act as stabilizing elements (Saumarez, 1986), limiting possible rib movement with ventilation. This acts to prevent the ribs, behaving as columns, from falling together like dominoes, and imparts rigidity, locking the ribs, similar to "construction with rigid frames and shear walls" in architectural terminology, conferring massive stability in the plane of the wall. This is aided by the absence of openings within the chest wall. The direction of fibers in the intercostal muscles, in two layers at right angles, resembles the herringbone weave pattern of the brickwork in Brunelleschi's double dome in the Dome of the Cathedral in Florence, which also contains intermediary struts.

Masonry domes usually rest on drums that contain buttresses or circumferential chains to manage the outward exertional forces. The human body partly supports its dome externally by the vertebral column, but also limits this problem as the torso is in effect made of two ellipsoids joined together with a short waist. The lower ellipsoid, which is the pelvis, also acts as a pressure vessel, but is used for the processes of micturition, defecation, parturition, coughing, and blowing. In this way, changing the torso into one ovoid pressure vessel minimizes the stresses present at the "rim" of any bell-shaped structure. One effect of the circumferential exertional forces, as in our analogy of masonry domes, could be the cause of the gradual but inevitable increase in antero-posterior diameter of the thorax with aging (Oskvig, 1999; Gayzik et al., 2008).

Rib cortical thickness data were also collected by Mohr et al. (2007). Their data regarding rib cortical measurements were independently similar to the cortical thickness measured in the present article, but limited to only ribs 3 and 7. Their work also demonstrated an increase in rib cortical thickness from superior to inferior (3rd to 7th ribs), and from internal to external cortices. The CT technique employed here is more refined than Mohr's radiological plate method, with direct measurements of cortical thickness instead of indirect measurements using image-filtering techniques to distinguish the cortices on radiography. CT is also more exact in that the slice thickness was 0.25 mm, in contrast to Mohr's 3-mm bone slices, and bone density could also be measured, which could not be done by Mohr et al.

The data in this article are consistent with the double-dome hypothesis with stress directly proportional to the radius and radial stress decreasing from internal to external surfaces. The inner rib cortex is thicker and denser than the outer cortex, with bone density and thickness increasing progressively from the second to the seventh rib, before diminishing to the tenth rib, mirroring chest diameter.

Limitations of the study include the fact that bone was modeled as a normal material when it is known to be both anisotropic and viscoelastic, i.e., it handles certain directions of stress better than others owing to the alignment of the Haversian systems, and that it reacts better to loads applied gradually. All modern CT scanner machines produce helical scans and, in contrast to their high transverse plane resolution, their axial resolution is limited by pitch size, which in effect

acts as the wavelength that can be used to determine resolution according to Abbe's principle. Abbe's resolution limit or "diffraction limit" states that the smallest distance that can be resolved between two lines is proportional to the wavelength, where the mechanical pitch becomes the wavelength, but can be improved by overlapping scans (Stelzer, 2002).

The data in this article confirm that surgical plating of ribs as fracture repair using plates and screws can be performed safely on ribs at all levels; however, this article indicates that it is imperative that the screw lengths are measured correctly in order to utilize the internal rib cortex, which is 33% thicker and has double the cortical density of the external rib cortex.

In summary, rib morphology is similar to an architectural double-shell dome, with two independent concentric structures tied by a series of interconnecting struts formed by the superior and inferior rib cortices and medulla and intercostal muscles, resulting in a middle layer that acts as a honeycomb between the inner and outer shells together with the intercostal muscles acting as stabilizing shear wall elements.

CONCLUSION

The chest behaves as a pressure- and weight-loaded thick-walled shell, with stresses induced by coughing leading to changes in the internal morphology of the ribs. The morphologically identical ribs of the neonate adapt to the stresses caused by coughing and breathing, resulting in changes in cortical thickness and bone density that mimic a double-shell dome. The thicker and stronger inner cortex should be utilized in any rib fracture fixation.

ACKNOWLEDGMENTS

The authors express their gratitude to the donor cadavers and their families who participated in the medical school cadaveric donation program, and to Mr. Peter Bentley-Brown for assistance with specimen preparation.

REFERENCES

- Ashkan M, Ahmad Y. 2010. Discontinuous double-shell domes through Islamic eras in the Middle East and Central Asia. *Nexus Netw J* 12:287-319.
- Bass SL, Saxon L, Daly RM, Robling AG, Seeman E, Stuckey S. 2002. The effect of mechanical loading on the size and shape of bone in pre-, peri-, and postpubertal girls: A study in tennis players. *J Bone Miner Res* 17:2274-2280.
- Cadet ER, Vorys GC, Rahman R, Park SH, Gardner TR, Lee FY, Levine WN, Bigliani LU, Ahmad CS. 2010. Improving bone density at the rotator cuff footprint increases supraspinatus tendon failure stress in a rat model. *J Orthop Res* 28:308-314.
- Casha AR, Manché A, Gauci M, Camilleri-Podesta MT, Schembri-Wismayer P, Sant Z, Gatt R, Grima JN. 2012. Placement of transsternal wires according to an ellipsoid pressure vessel model of sternal forces. *Interact Cardiovasc Thorac Surg* 14:283-287.
- Casha AR, Manché A, Gatt R, Duca E, Gauci M, Schembri-Wismayer P, Sant Z, Gatt R, Grima JN. 2014. Mechanism of sternotomy dehiscence. *Interact Cardiovasc Thorac Surg* 19:617-621.

- Casha AR, Camilleri L, Manché A, Gatt R, Attard D, Gauci M, Camilleri-Podesta' MT, Grima JN. 2015. External rib structure can be predicted using mathematical models: An anatomical study with application to understanding fractures and intercostal muscle function. *28*:512–519. *Clin Anat*
- Dai QG, Liu YK. 1992. Failure analysis of a beam-column under oblique-eccentric loading: Potential failure surfaces for cervical spine trauma. *J Biomech Eng* 114:119–128.
- Farshad M. 1977. On the shape of momentless tensionless masonry domes. *J Build Environ* 12:81–85.
- Gayzik FS, Yu MM, Danelson KA, Slice DE, Stitzel DE. 2008. Quantification of age-related shape change of the human rib cage through geometric morphometrics. *J Biomech* 41:1545–1554.
- Hejazi M. 2003. Seismic vulnerability of Iranian historical domes. In: Latini G, Brebbia CA, editors. *Advances in Earthquake Engineering, Earthquake Resistant Engineering Structures IV*. Southampton: WIT Press. p 157–165.
- Hillenbrand R. 1994. *Islamic Architecture: Form, Function, and Meaning*. New York: Columbia University Press. p 1–645.
- Huerta S. 2006. Geometry and equilibrium: The gothic theory of structural design. *Struct Eng* 84:23–28.
- Huiskes R. 2000. If bone is the answer, then what is the question? *J Anat* 197:145–156.
- Michell G. 1984. *Architecture of the Islamic World: Its History and Social Meaning*. New York: Thames and Hudson. p 1–288.
- Misztal B. 2010. Domes in architecture. *Architectus* 2:289–293.
- Mohr M, Abrams E, Engel C, Long WB, Bottlang M. 2007. Geometry of human ribs pertinent to orthopedic chest-wall reconstruction. *J Biomech* 40:1310–1317.
- Oskvig RM. 1999. Special problems in the elderly. *Chest* 115:158S–164S.
- Pal GP, Routal RV. 1986. A study of weight transmission through the cervical and upper thoracic regions of the vertebral column in man. *J Anat* 148:245–261.
- Pal GP, Routal RV. 1987. Transmission of weight through the lower thoracic and lumbar regions of the vertebral column in man. *J Anat* 152:93–105.
- Parnas L, Katirci N. 2002. Design of fiber-reinforced composite pressure vessels under various loading conditions. *Compos Struct* 58:83–95.
- Pender DJ. 2009. A model analysis of static stress in the vestibular membranes. *Theor Biol Med Model* 6:19.
- Pontrelli G. 2002. A mathematical model of flow through a viscoelastic tube. *Med Biol Eng Comput* 40:550–556.
- Robling AG, Hinant FM, Burr DB, Turner CH. 2002. Improved bone structure and strength after long-term mechanical loading is greatest if loading is separated into short bouts. *J Bone Miner Res* 17:1545–1554.
- Ruff C, Holt B, Trinkaus E. 2006. Who's afraid of the big bad wolff?: "Wolff's law" and bone functional adaptation. *Am J Phys Anthropol* 129:484–498.
- Saumarez RC. 1986. An analysis of action of intercostal muscles in human upper rib cage. *J Appl Physiol* 60:690–701.
- Stelzer EHK. 2002. Light microscopy: Beyond the diffraction limit? *Nature* 417:806–807.
- Talbert TG. 2005. Paroxysmal cough injury, vascular rupture and "shaken baby syndrome." *Med Hypotheses* 64:8–13.
- Young WC, Budynas RG. 2002. *Roark's Formulas for Stress and Strain*. New York: McGraw-Hill. p 1–852.